
# Local Surface Plasmon-Graphene Synergy for Efficient Quantum Dot Color Conversion in Micro-LEDs

Downloaded from: https://research.chalmers.se, 2026-02-04 18:45 UTC

Citation for the original published paper (version of record):
Fang, A., Li, Q., Liu, J. et al (2025). Local Surface Plasmon-Graphene Synergy for Efficient Quantum Dot Color Conversion in Micro-LEDs. ACS Photonics, 12(11): 6300-6307.
http://dx.doi.org/10.1021/acsphotonics.5c01788

N.B. When citing this work, cite the original published paper.

research.chalmers.se offers the possibility of retrieving research publications produced at Chalmers University of Technology. It covers all kind of research output: articles, dissertations, conference papers, reports etc. since 2004. research.chalmers.se is administrated and maintained by Chalmers Library

(article starts on next page)

ACS Photonics

Open Access

This article is licensed under CC-BY 4.0

pubs.acs.org/journal/apchd5

Article

# Local Surface Plasmon–Graphene Synergy for Efficient Quantum Dot Color Conversion in Micro-LEDs

Aoqi Fang, Qingqing Li, Jixin Liu, Zaifa Du, Penghao Tang, Hao Xu, Rongjing Wang, Jibin Song, Qun Yan, Weiling Guo,* and Jie Sun*

Cite This: *ACS Photonics* 2025, 12, 6300–6307

Read Online

ACCESS | Metrics & More | Article Recommendations | Supporting Information

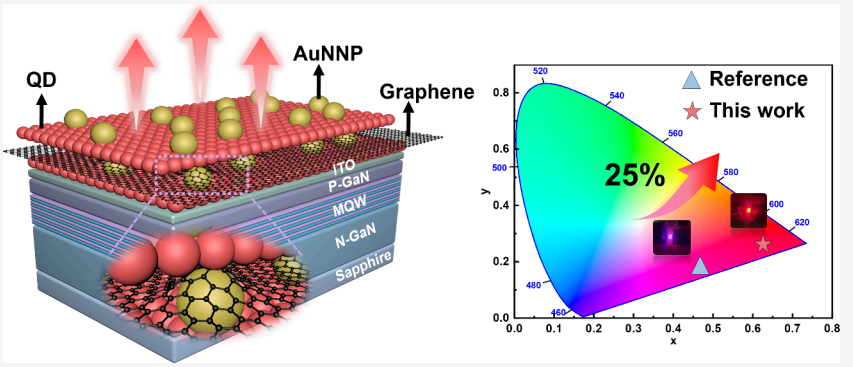


**ABSTRACT:** Exciting quantum dots (QDs) with short-wavelength micro-LEDs (μLEDs) are one of the most promising approaches for achieving full-color μLED displays. However, the low color conversion efficiency (CCE) caused by surface carrier loss in QDs remains a major barrier to large-scale application. In this work, we propose a novel color conversion layer structure incorporating a graphene interlayer and nanogapped gold nanoparticles (AuNNPs) within the QD layer to realize efficient color conversion in GaN-based blue μLEDs. The AuNNPs can boost the radiative recombination of the QDs via localized surface plasmon resonance (LSPR), which further improves the quantum yield. Meanwhile, the graphene layer functions as a carrier transport channel, facilitating the transfer of photogenerated carriers to adjacent QDs, thereby promoting the carrier population and radiative recombination within the QDs. Detailed physical analysis and optical measurements confirm the feasibility of this strategy. The results show that the synergistic effects of AuNNPs and graphene enable a high CCE of over 91%, with a 25% improvement compared to conventional structures at a current density of 200 A/cm$^2$. This QD/AuNNP-Graphene-QD/AuNNP multilayer structure demonstrates significant potential for full-color display applications in μLED technology.

**KEYWORDS:** *micro-LED, graphene, local surface plasmon, quantum dot, nanoparticle*

Downloaded via CHALMERS UNIV OF TECHNOLOGY on December 30, 2025 at 11:46:35 (UTC).
See https://pubs.acs.org/sharingguidelines for options on how to legitimately share published articles.

## INTRODUCTION

In conventional micro light-emitting-diode (μLED) display arrays, full-color emission is typically achieved by heterogeneously integrating blue, green, and red μLEDs onto a driving substrate.[1,2] However, this heterogeneous integration process is inherently complex, and the postintegration device yield remains suboptimal. In particular, the low external quantum efficiency of AlGaInP-based red μLEDs and their integration compatibility with GaN-based blue and green μLEDs present significant challenges.[3,4]

Compared with such a heterogeneous integration scheme, employing quantum dot (QD) color conversion layers to realize full-color μLED displays has emerged as a more practical and promising approach and has become a major research focus in the μLED display field.[5−7] Nevertheless, in both flip-chip and vertical configurations, the QD layer is typically separated from the multiple quantum well (MQW) layer of the μLED by a distance ranging from hundreds of nanometers to several micrometers.[8,9] This spatial separation results in substantial photon loss before absorption by the QDs. Moreover, intrinsic defect states in QDs can further cause nonradiative recombination of photogenerated carriers, thereby significantly reducing the photon energy utilization efficiency, and ultimately limiting the performance of QD-based full-color μLED displays.[10,11]

To address these issues, various structural optimizations have been proposed, such as introducing nanoholes,[12]

Received: July 27, 2025
Revised: September 29, 2025
Accepted: September 30, 2025
Published: October 13, 2025

© 2025 The Authors. Published by American Chemical Society

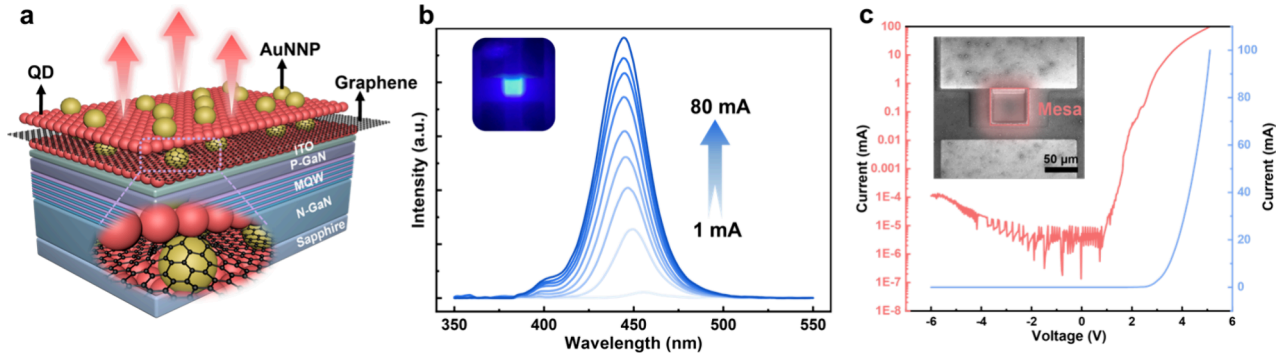


**Figure 1.** (a) Schematic diagram of the μLED-QD-AuNNP-Gr structure, (b) EL spectrum and emission image of the blue μLED, and (c) SEM image and I–V characteristics of the μLED with the QD layer.

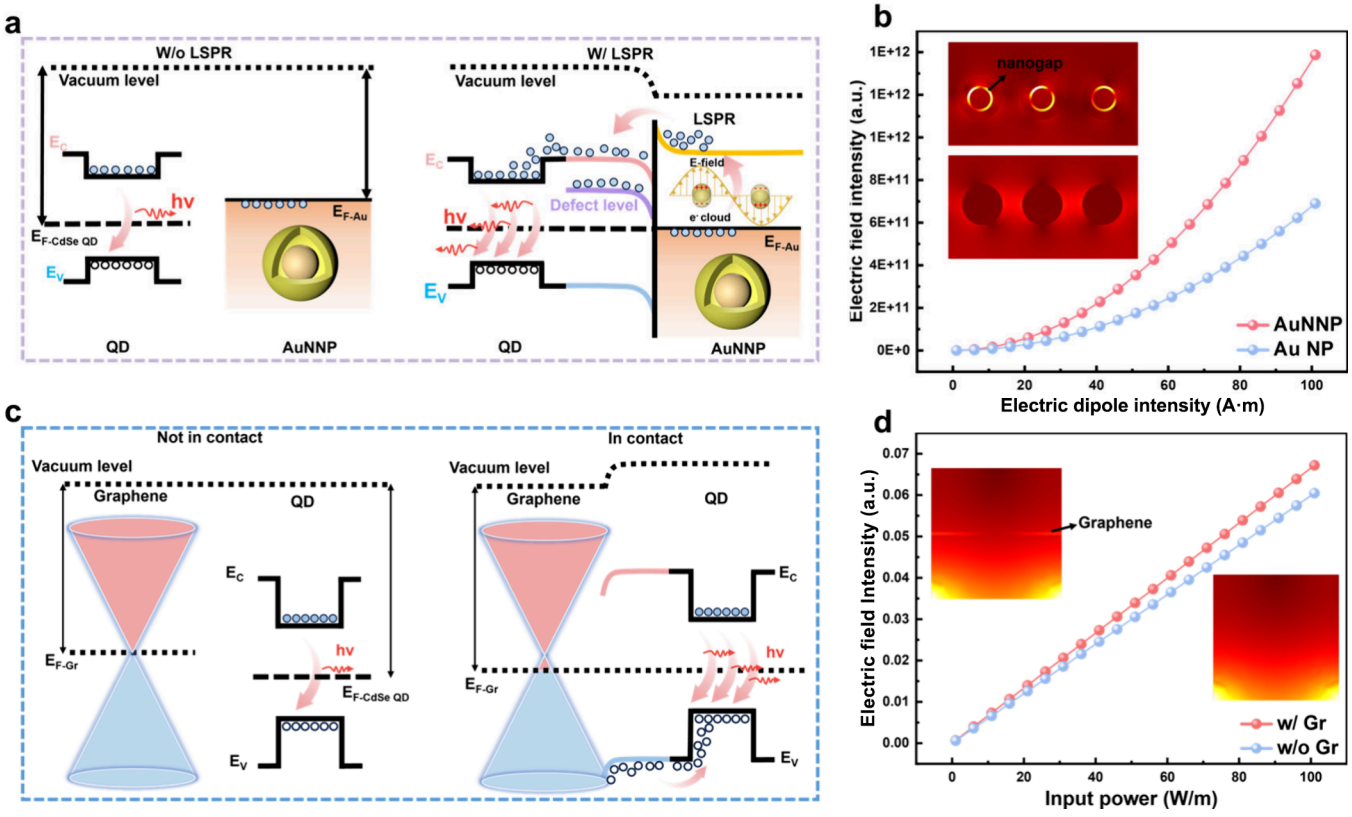


**Figure 2.** (a) Energy band diagram and carrier transfer path schematic in the LSPR system. (b) Simulated electric field distribution in the QD layer for Au nanoparticles with (AuNNP) and without (Au NP) nanogap structures. (c) Energy band diagram and carrier transfer path schematic before and after contact between graphene and QDs, and (d) simulated electric field distribution in the QD layer with a graphene layer.

nanorods,[13] and nanorings,[14] which can enhance QD color conversion efficiency (CCE) via nonradiative energy transfer (NRET). However, the incorporation of such nanostructures increases fabrication complexity and challenges large-scale production. Increasing the QD layer thickness is another strategy to improve CCE, but it often comes at the expense of reduced overall luminous efficiency.[15,16] In contrast, incorporating nanomaterials directly into the QD layer offers a more compatible and feasible solution. This approach can enhance the CCE while maintaining process simplicity and luminous efficiency. Several studies have confirmed that mixing metal nanoparticles with QDs can enhance radiative recombination through localized surface plasmon resonance (LSPR), enabling efficient light absorption and color conversion.[17,18] Additionally, graphene, owing to its ultrahigh carrier mobility and broad-spectrum absorption, has been widely used in photodetectors as both a carrier transport and light absorption layer.[19,20] Recent reports further demonstrate that photogenerated carriers in graphene can be effectively transferred to QDs, thereby positively contributing to photoluminescence emission.[21,22]

To address the aforementioned challenges, we assembled a QD layer incorporating both nanogapped gold nanoparticles (AuNNPs) and a graphene intercalation layer on the emission surface of a GaN-based blue μLED (μled-QD-AuNNP-Gr). In this structure, the μLED serves as the excitation light source, while the AuNNPs—featuring nanogaps—are designed with plasmon resonance peaks matched to the QD emission wavelength (≈630 nm). Both numerical simulations and experimental investigations were conducted to explore the


https://doi.org/10.1021/acsphotonics.5c01788
ACS Photonics 2025, 12, 6300−6307

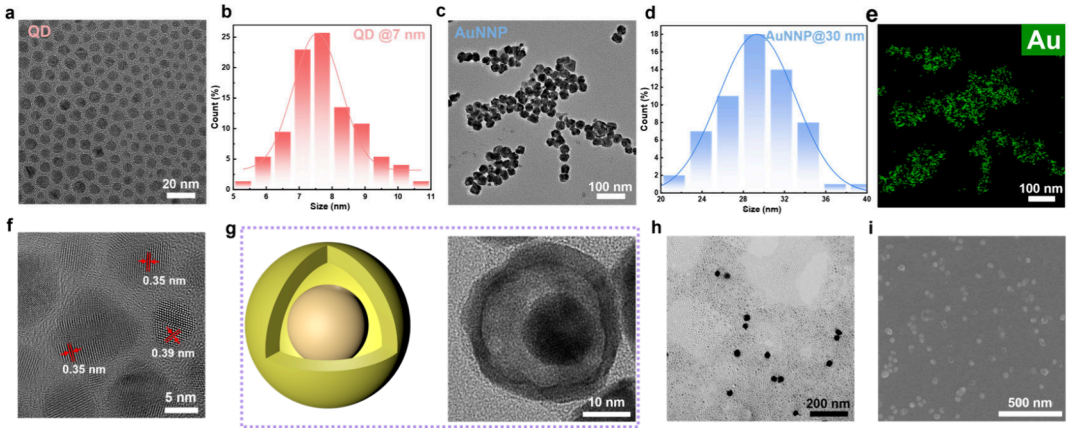


**Figure 3.** (a and b) TEM images of QDs and their size distribution and (c and d) TEM images of AuNNPs and their size distribution. (e) EDS spectrum of AuNNPs. (f) Lattice structure of QD at super-resolution magnification. (g) Structural schematic of an AuNNP, along with a TEM image of a single AuNNP and (h) QD/AuNNP. (i) SEM image of QD/AuNNP spin-coated on the $\mu$LED surface.

effects of this hybrid design on the QD absorption and emission. Theoretical analysis and experimental results consistently confirm that LSPR, along with carrier transfer between graphene and QDs, plays a positive role in enhancing the QD emission. Experimentally, under the condition of maintaining excellent electrical performance, the $\mu$LEDs integrated with both AuNNPs and the graphene interlayer exhibited a remarkably high CCE. Specifically, when only the AuNNPs or graphene interlayer were individually incorporated into the QD layer, the CCE reached 90% and 85%, respectively, under an injection current density of 100 A/cm$^2$. These represent improvements of 23% and 16% compared to conventional QD-integrated $\mu$LEDs, respectively. When both components were simultaneously present, the CCE further increased to 92%, marking a 25% enhancement. Moreover, this improvement continues to increase with higher current densities.

## EXPERIMENTAL SECTION

Figure 1(a) illustrates a schematic diagram of our $\mu$LED-QD-AuNNP-Gr structure. Figure 1(b) shows the electroluminescence (EL) spectrum and emission image of the GaN-based $\mu$LED used as the excitation source. Figure 1(c) presents the electrical characteristics and scanning electron microscopy (SEM) image of the $\mu$LED after spin-coating the QDs. We employed commercially available GaN-on-sapphire epitaxial wafers, and the thickness of the p-GaN layer is 105 nm. To ensure a good ohmic contact between the metal electrode and the p-GaN layer, a 110 nm-thick indium tin oxide layer was deposited on the p-GaN surface. This results in a vertical separation exceeding 200 nm between the MQW layer and the QD layer. The $\mu$LED devices were fabricated by using standard LED processing techniques. The detail fabrication process is provided in the Supporting Information (Figure S1). After the $\mu$LED fabrication, the QDs/AuNNPs mixture was uniformly spin-coated onto the $\mu$LED surface. A monolayer of graphene was then transferred onto the QD/AuNNP layer using a wet transfer process. Following this, a second QD/AuNNP layer was spin-coated on top. The detailed procedures for spin-coating and graphene transfer are described in the Supporting Information (Figure S2 and Figure S3).

## MECHANISM ANALYSIS

When the distance between the AuNNPs and QDs is less than 100 nm and the absorption peak of AuNNPs highly overlaps with the emission wavelength of the QDs, a strong local electric field can be generated around the AuNNPs upon excitation of the QDs. The collective oscillation of free electrons in the AuNNPs (surface plasmons) resonantly couples with the incident light and transfers energy to the QDs, thereby enhancing their emission intensity.[23,24] In addition, excited electrons on the surface of the AuNNPs may transfer into the conduction band or defect states of the QDs, where they can recombine radiatively with holes in the valence band, resulting in photon emission. In Figure 2(a), we illustrate the mechanism of electronic state modulation at the QD−Au interface.[25,26] In Figure 2(b), we present simulation results of the LSPR effect of AuNNPs. The electric field intensity near the nanoparticles is significantly higher than in other regions, indicating the positive role of LSPR in field enhancement. Notably, the nanogap region in the AuNNPs exhibits particularly strong field enhancement, which is a key reason we selected this specific nanostructure design. As shown in Supporting Information Figure S4, the absorption resonance peak of the AuNNPs is closer to the emission wavelength of the QDs compared with that of conventional AuNPs of the same size, which is more favorable for enhancing the LSPR strength.

Figure 2(c) illustrates the band bending and carrier transfer that occur upon contact between the graphene and QDs. Graphene, being a two-dimensional semimetal with high carrier mobility, forms a charge transfer interface with QDs due to the work function difference when they come into contact. This charge transfer induces band bending and creates a built-in electric field at the interface. Upon photon absorption, graphene generates electron−hole pairs, and the built-in electric field directs the photogenerated carriers toward the QDs.[21,22,27] According to the radiative recombination rate formula in QDs (eq 1),

$$R_{rad} = B \times n \times p \tag{1}$$

where $R_{rad}$ is the radiative recombination rate, $B$ is the radiative recombination coefficient, and $n$ and $p$ are the electron and hole concentrations, respectively. This equation indicates that the radiative recombination rate positively correlates with the


https://doi.org/10.1021/acsphotonics.5c01788
ACS Photonics 2025, 12, 6300−6307

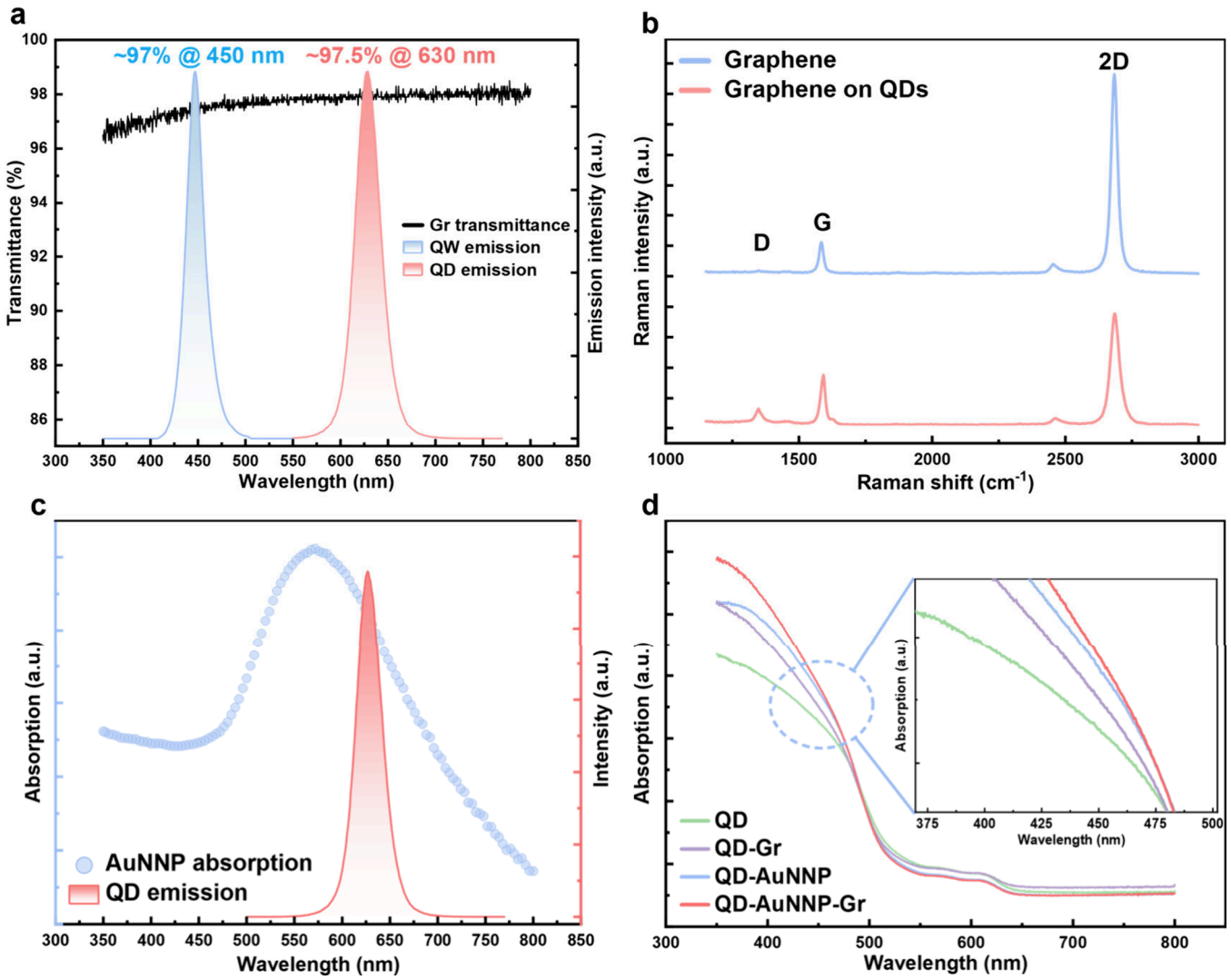


**Figure 4.** (a) Transmittance at different wavelengths, (b) Raman spectrum of the graphene used in the experiment, (c) absorption spectra of the AuNNPs used in the experiment at different wavelengths, and (d) absorption spectra of QD layers with different structures.

carrier concentration. After photogenerated carriers are transferred from graphene to the QDs, the radiative recombination rate in the QDs increases, leading to an enhanced emission intensity. Furthermore, carriers transferred from graphene can fill defect states in the QDs, thereby reducing nonradiative recombination and further increasing the proportion of radiative recombination. In Figure 2(d), we performed simulations of QDs with a graphene insertion layer and observed that graphene enhances the local electric field intensity around it. This enhancement is crucial for QDs located farther from the excitation source.

## RESULTS AND DISCUSSION

The QDs used in this study are CdSe/ZnS core−shell spherical nanoparticles with an average diameter of approximately 7 nm. Figure 3(a) and (d) presents the transmission electron microscopy (TEM) images of the QDs and AuNNPs and their particle size distributions used in this study, respectively. Figure 3(b) and (d) shows their corresponding particle size distribution. Figure 3(e) shows the corresponding energy dispersive spectrometer (EDS) spectrum of AuNNPs, and Figure 3 (f) shows the lattice structure of QDs at ultrahigh resolution magnification. The structure of a single AuNNP is shown in Figure 3(g), which is a Au−Air−Au structure consisting of an internal Au core, an air gap layer, and an external gold shell. After thorough ultrasonic mixing of the QDs and AuNNPs, the AuNNPs are uniformly dispersed within the QD matrix, as shown in the TEM images of the QDs/AuNNPs hybrid in Figures 3(h). Following spin-coating of the hybrid QDs/AuNNPs layer onto the $\mu$LED mesa, the surface morphology was characterized by SEM, as shown in Figure 3(i). The SEM image confirms the uniform distribution of AuNNPs within the QD layer, which is one of the fundamental prerequisites for the uniform excitation of the LSPR throughout the QD layer.

The transmittance spectrum of the monolayer graphene used in this experiment is shown in Figure 4(a). The optical transmittance reaches approximately 97% at both the emission wavelength of the $\mu$LED (≈450 nm) and that of the QDs (≈630 nm), indicating minimal optical loss as photons pass through the graphene. We attribute this slight loss to photon absorption in graphene, which primarily contributes to the generation of photogenerated carriers. Figure 4(b) presents the Raman spectra of the graphene layer before and after being transferred to the QD layer. The intensity ratio of the 2D and D peaks confirms that the transferred graphene is most likely


https://doi.org/10.1021/acsphotonics.5c01788
ACS Photonics 2025, 12, 6300−6307

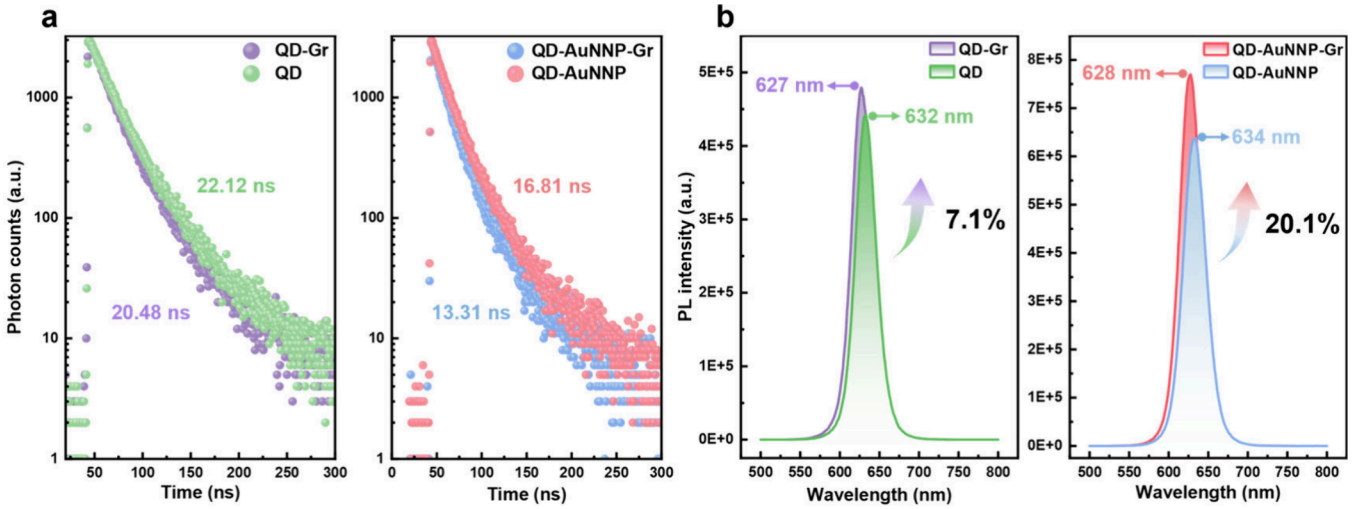


**Figure 5.** (a) TRPL and (b) PL spectra of QD layers with four different structures.

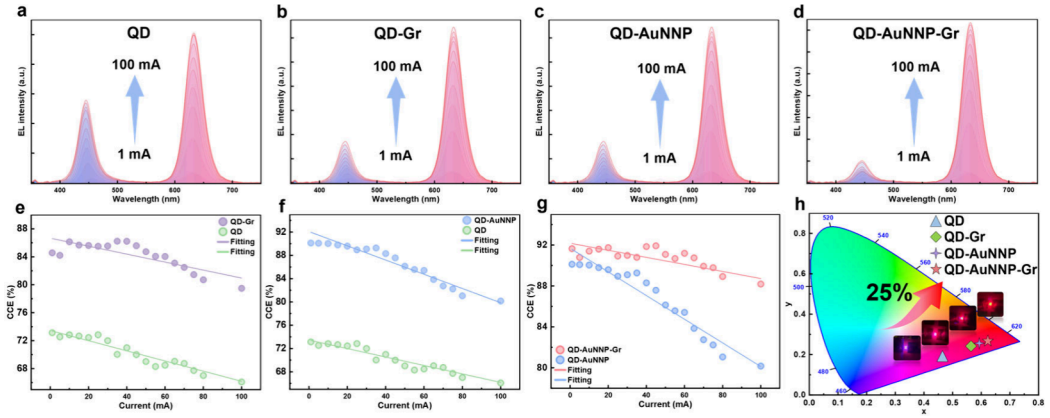


**Figure 6.** $\mu$LEDs with QD layers of four different structures. (a–d) EL spectra; (e–g) CCE under different injection currents. (h) CIE 1931 chromaticity coordinates at 10 mA injection current.

monolayer graphene.[28] A slight increase in the D peak after transfer suggests the introduction of defects, likely caused by contamination during the transfer process such as residual PMMA or impurities within the QD layer. The absorption spectrum of the AuNNPs is shown in Figure 4(c), where a pronounced absorption peak is observed in the emission range of the QDs. This strong spectral overlap is one of the necessary conditions for LSPR coupling between the AuNNPs and QDs.[23,24] Figure 4(d) displays the absorption spectra of the different QD layers. With the sequential addition of AuNNPs and a graphene interlayer, the absorption intensity in the blue wavelength range increases accordingly. This observation supports the reliability of the proposed mechanisms of carrier transfer from graphene to QDs and plasmonic enhancement due to LSPR, as directly evidenced by the enhanced QD absorption.

To further investigate the enhancement effects of AuNNPs and graphene on QDs, we performed photoluminescence (PL) and time-resolved photoluminescence (TRPL) measurements on different types of QD layers. As shown in Figure 5(a), the TRPL results reveal that, after the introduction of graphene, the PL decay times of QD layers with and without AuNNPs decreased from 22.12 and 16.81 ns to 20.48 and 13.31 ns, respectively. This indicates an accelerated rate of recombination of carriers within the QDs, which we attribute to carrier transfer from graphene to the QDs. Similarly, due to the enhancement effect of LSPR, the QD layers containing AuNNPs also exhibit significantly shorter PL decay times compared to those without AuNNPs. The reduction in PL decay time confirms an improvement in the carrier recombination efficiency within the QDs, which is further reflected in the enhanced PL intensity, as shown in Figure 5(b). Additionally, we observed a blue shift of approximately 5–6 nm in the PL emission peak of QD layers incorporating graphene. This shift is likely due to the introduction of new energy states at the QD–graphene interface. The presence of these additional energy levels allows excited electrons in the QDs to transition to intermediate energy states in the nearby graphene before radiative recombining to the ground state. This process increases the energy difference during radiative recombination, thereby resulting in the emission of higher-energy (shorter-wavelength) photons.[29] Alternatively, this blue shift may also arise from protonation of the QD surface, which can be induced by a decrease in the pH of the QD layer during the graphene transfer process.[30,31]

Figure 6(a)–(d) presents the EL spectra of $\mu$LEDs with different QD layer configurations. It is evident that following the introduction of both the graphene interlayer and AuNNPs, the intensity ratio of the red emission peak (from QDs) to the blue emission peak (from the $\mu$LED) increases progressively.


https://doi.org/10.1021/acsphotonics.5c01788
ACS Photonics 2025, 12, 6300–6307

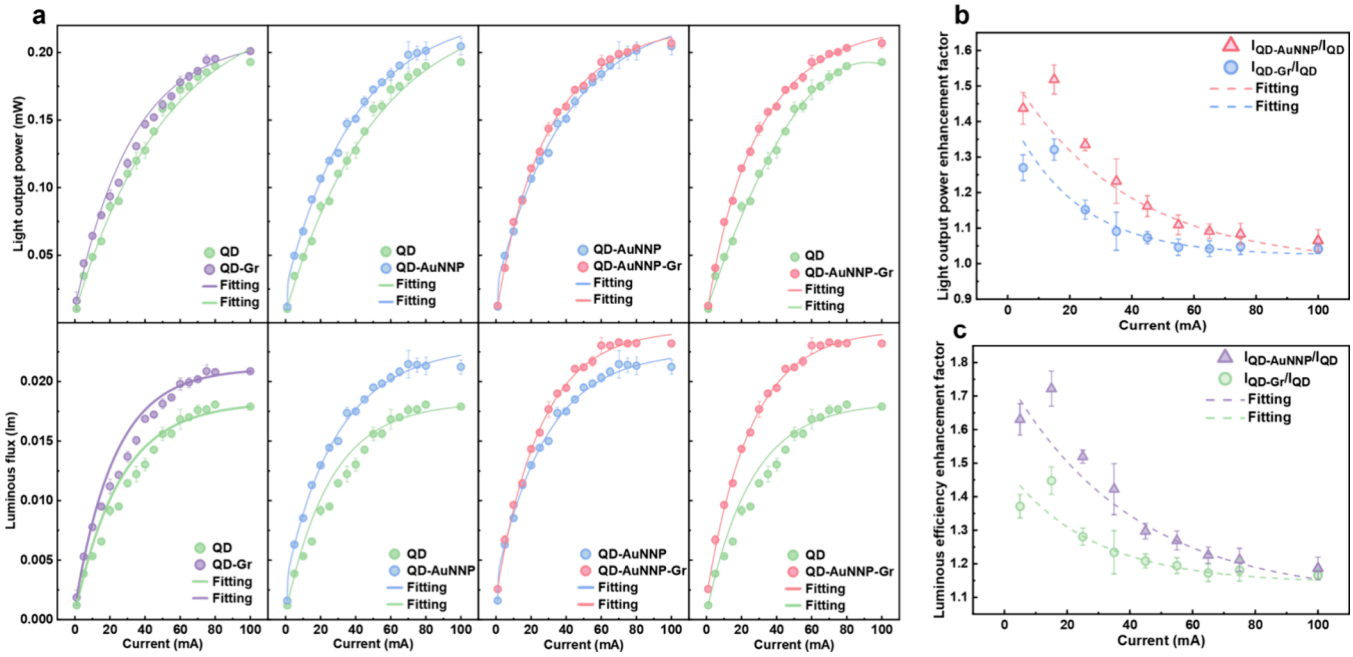


**Figure 7.** (a) Comparison of light output power and luminous flux of $\mu$LEDs with QD layers of four different structures and enhancement factors of (b) light output power and (c) luminous flux for $\mu$LED-QD-AuNNPs and $\mu$LED-QD-Gr.

This indicates that the efficiency with which QDs utilize high-energy photons emitted by the $\mu$LED is notably enhanced. This enhancement arises from the contributions of LSPR and photoinduced carrier transfer from graphene, both of which facilitate more efficient photon conversion within the QD layer. When both mechanisms are present, the enhancement becomes more pronounced. To quantitatively evaluate the energy conversion efficiency of the $\mu$LED emission by the QD layer in different configurations, we introduce the CCE, which is calculated using Equation 2:

$$CCE = \frac{\int_{QD_{emission}} \left(\frac{\lambda}{hc}\right) \times [I_{QD}(\lambda)]d\lambda}{\int_{QW,QD_{emission}} \left(\frac{\lambda}{hc}\right) \times [I_{QW}(\lambda) + I_{QD}(\lambda)]d\lambda} \quad (2)$$

where $I_{QD}$ and $I_{QW}$ are the emission intensities of the QD and QW in the EL spectrum. The calculated CCE under different injection currents for each device structure is shown in Figure 6(e)−(g). It is evident that the introduction of either a AuNNPs or graphene interlayer into the QD layer significantly improves the CCE, with enhancements of 23% and 16%, respectively. Notably, the QD layer incorporating the graphene interlayer exhibits a superior stability at higher injection currents. This is attributed to the excellent thermal conductivity of graphene, which enables more uniform heat dissipation across the QD layer, thereby maintaining consistent absorption and emission behavior under high current densities. The color performance of the $\mu$LEDs at 10 mA with various QD configurations is mapped on the International Commission on Illumination (CIE) 1931 chromaticity diagram in Figure 6(h), providing an intuitive comparison of the emission characteristics across different device structures. Compared with the conventional QD layer, the QD-AuNNP-Gr layer structure exhibited a 25% increase in CCE.

Figure 7(a) compares the light output power and luminous flux of QD-$\mu$LEDs with those of four distinct QD layer configurations. Devices incorporating both AuNNP and the graphene interlayer demonstrate superior optical performance. The enhancement primarily arises from LSPR, which significantly improves QD absorption, radiative recombination, and emission. Additionally, photogenerated carrier transfer from graphene to QDs contributes to the overall emission enhancement. Figure 7(b) and (c) show the enhancement factors for light output power and luminous flux when AuNNPs or graphene is individually introduced into the QD layer. The data clearly indicate that AuNNPs exert a more pronounced effect, underscoring the dominant role of LSPR in this system.

## CONCLUSION

By incorporating metal nanoparticles and a graphene interlayer into the QD layer, we significantly enhanced the CCE of the QD layer in QD-based $\mu$LEDs through LSPR and carrier transfer mechanisms. The CCE peak reached over 92%, representing a 25% improvement compared with conventional QD-only layers. This simple approach does not require any structural modification of the device, making it suitable for large-scale $\mu$LED color conversion and practical manufacturing. Our work provides a valuable reference for future full-color $\mu$LED display technologies.

## ASSOCIATED CONTENT

### Data Availability Statement

The data that support the findings of this study are available from the corresponding author upon reasonable request.

### Supporting Information

The Supporting Information is available free of charge at https://pubs.acs.org/doi/10.1021/acsphotonics.5c01788.

Preparation processes of $\mu$LED-QD-AuNNP-Gr; QDs/AuNNPs spin-coating process and the AFM images of deposited QDs/AuNNPs; graphene transfer steps; preparation process of AuNNP; comparison of the absorption spectra of different materials and structures;



https://doi.org/10.1021/acsphotonics.5c01788
ACS Photonics 2025, 12, 6300−6307

EL spectra and corresponding CIE 1931 chromaticity diagrams of QD-μLEDs without and with AuNNP−graphene hybrid layers (PDF)

## AUTHOR INFORMATION


### Corresponding Authors

**Weiling Guo** − *Key Laboratory of Optoelectronics Technology, Beijing University of Technology, Beijing 100124, China*; Email: guoweiling@bjut.edu.cn

**Jie Sun** − *Fujian Science and Technology Innovation Laboratory for Optoelectronic Information of China, and College of Physics and Information Engineering, Fuzhou University, Fuzhou 350100, China; Quantum Device Physics Laboratory, Department of Microtechnology and Nanoscience, Chalmers University of Technology, Gothenburg 41296, Sweden*; orcid.org/0000-0002-6479-7771; Email: jie.sun@fzu.edu.cn

### Authors

**Aoqi Fang** − *Key Laboratory of Optoelectronics Technology, Beijing University of Technology, Beijing 100124, China*; orcid.org/0009-0006-9297-9296

**Qingqing Li** − *College of Chemistry, Chemical Engineering and Materials Science, Collaborative Innovation Center of Functionalized Probes for Chemical Imaging in Universities of Shandong, Key Laboratory of Molecular and Nano Probes, Ministry of Education, Shandong Normal University, Jinan 250014, China*

**Jixin Liu** − *Key Laboratory of Optoelectronics Technology, Beijing University of Technology, Beijing 100124, China*

**Zaifa Du** − *School of Physics and Electronic Information, Weifang University, Weifang 261061, China*; orcid.org/0000-0002-4269-5504

**Penghao Tang** − *Key Laboratory of Optoelectronics Technology, Beijing University of Technology, Beijing 100124, China*

**Hao Xu** − *Key Laboratory of Optoelectronics Technology, Beijing University of Technology, Beijing 100124, China*

**Rongjing Wang** − *Key Laboratory of Optoelectronics Technology, Beijing University of Technology, Beijing 100124, China*

**Jibin Song** − *State Key Laboratory of Chemical Resource Engineering, College of Chemistry, Beijing University of Chemical Technology, Beijing 10010, China*; orcid.org/0000-0003-4771-5006

**Qun Yan** − *Fujian Science and Technology Innovation Laboratory for Optoelectronic Information of China, and College of Physics and Information Engineering, Fuzhou University, Fuzhou 350100, China*

Complete contact information is available at: https://pubs.acs.org/10.1021/acsphotonics.5c01788



### Funding

This work was supported by National Key Research and Development Program of China (2023YFB3608703 and 2023YFB3608700), National Natural Science Foundation of China (12474066), Fujian Science & Technology Innovation Laboratory for Optoelectronic Information of China (2021ZZ122 and 2020ZZ110), and Wuhan municipal project (2024010702020024).


### Notes

The authors declare no competing financial interest.

## REFERENCES


(1) Li, Y.; Tao, J.; Zhao, Y.; Wang, J.; Lv, J.; Qin, Y.; Liang, J.; Wang, W. 48 × 48 pixelated addressable full-color micro display based on flip-chip micro LEDs. *Appl. Opt.* **2019**, *58*, 8383−8389.

(2) Li, P.; Zhang, X.; Qi, L.; Lau, K. Full-color micro-display by heterogeneous integration of InGaN blue/green dual-wavelength and AlGaInP red LEDs. *Opt. Express* **2022**, *30*, 23499−23510.

(3) Qi, L.; Li, P.; Zhang, X.; Wong, K.; Lau, K. Monolithic full-color active-matrix micro-LED micro-display using InGaN/AlGaInP heterogeneous integration. *Light Sci. Appl.* **2023**, *12*, 258.

(4) Kang, C.; Lee, J.; Kong, D.; Shim, J.; Kim, S.; Mun, S.; Choi, S.; Park, M.; Kim, J.; Lee, D. Electrically driven full-color single-chip microdisplay using quantum dots patterned by photoresist. *ACS Photonics* **2018**, *5* (11), 4413−4422.

(5) Ma, T.; Chen, J.; Chen, Z.; Liang, L.; Hu, J.; Shen, W.; Li, Z.; Zeng, H. Progress in color conversion technology for micro-LED. *Adv. Mater. Technol.* **2023**, *8*, No. 2200632.

(6) Weng, Y.; Chen, G.; Zhou, X.; Zhang, Y.; Yan, Q.; Guo, T. Design and fabrication of patterned high performance quantum-dot color conversion films for μLED full color display applications. *J. Lumin.* **2023**, *261*, No. 119892.

(7) Liang, K.; Kuo, W.; Shen, H.; Lin, S.; Fang, Y.; Lai, Y.; Lin, C. Highly efficient fine-pitch quantum dot/titanium oxide nanocomposites for ultrahigh-resolution full-color micro-light emitting diode displays. *ACS Photonics* **2024**, *11* (8), 2981−2991.

(8) Guo, Y.; Yu, J.; Huang, L.; Liu, Z.; Gai, Z.; Zhi, T.; Zhou, Y.; Tao, T.; Liu, B.; Zhang, R.; Zheng, Y. Monolithic full-color micro-LED displays featuring three-dimensional chip bonding and quantum dot-based color conversion layer. *Opt. Express* **2024**, *32*, 27662−27669.

(9) Qi, L.; Zhang, X.; Chong, W.; Lau, K. Monolithically integrated high-resolution full-color GaN-on-Si micro-LED microdisplay. *Photon. Res.* **2023**, *11*, 109−120.

(10) Huang, Y.; Chen, J.; Liou, Y.; James Singh, K.; Tsai, W.; Han, J.; Lin, C.; Kao, T.; Lin, C.; Chen, S.; et al. High-uniform and high-efficient color conversion nanoporous GaN-based micro-LED display with embedded quantum dots. *Nanomaterials* **2021**, *11* (10), 2696.

(11) Fan, X.; Wu, T.; Liu, B.; Zhang, R.; Kuo, H.; Chen, Z. Recent developments of quantum dot based micro-LED based on non-radiative energy transfer mechanism. *Opto-Electron. Adv.* **2021**, *4*, No. 210022.

(12) Du, Z.; Li, D.; Guo, W.; Xiong, F.; Tang, P.; Zhou, X.; Zhang, Y.; Guo, T.; Yan, Q.; Sun, J. Quantum dot color conversion efficiency enhancement in micro-light-emitting diodes by non-radiative energy transfer. *IEEE Electron Device Lett.* **2021**, *42* (8), 1184−1187.

(13) Fang, A.; Tang, P.; Xie, Y.; Du, Z.; Guo, W.; Mei, Y.; Xu, H.; Sun, J. High color conversion efficiency realized in graphene-connected nanorod micro-LEDs using hybrid Ag nanoparticles and quantum dots. *Adv. Opt. Mater.* **2024**, *12*, No. 2400230.

(14) Huang Chen, S.; Shen, C.; Wu, T.; Liao, Z.; Chen, L.; Zhou, J.; Lee, C.; Lin, C.; Lin, C.; Sher, C.; Lee, P.; Tzou, A.; Chen, Z.; Kuo, H. Full-color monolithic hybrid quantum dot nanoring micro light-emitting diodes with improved efficiency using atomic layer deposition and nonradiative resonant energy transfer. *Photon. Res.* **2019**, *7*, 416−422.

(15) Lin, Y.; Huang, W.; Zhanghu, M.; Liu, Z. Ultra-thick inkjet-printed quantum dots layer for full-color micro-LED displays. *Opt. Express* **2023**, *31*, 31818−31824.

(16) Hyun, B.; Sher, C.; Chang, Y.; Lin, Y.; Liu, Z.; Kuo, H. Dual role of quantum dots as color conversion layer and suppression of input light for full-color micro-LED displays. *J. Phys. Chem. Lett.* **2021**, *12* (29), 6946−6954.

(17) Lai, Y.; Yang, S.; Feng, H.; Lee, Y.; Li, Z.; Wu, S.; Lin, Y.; Hsieh, H.; Chu, C.; Chen, W.; et al. Surface plasmon coupling effects on the photon color conversion behaviors of colloidal quantum dots in a GaN nanoscale hole with a nearby quantum-well structure. *Opt. Express* **2023**, *31*, 16010−16024.

(18) Jang, J.; Cho, H.; Choi, S.; Jeon, H.; Kang, C.; Kim, Y.; Kang, H.; Hahm, D.; Kim, J.; Jeong, J.; et al. Highly enhanced light recycling

in quantum dot displays by sidewall reflectors. *Adv. Opt. Mater.* **2025**, *13*, No. 2402147.
(19) Hu, L.; Dong, Y.; Xie, Y.; Qian, F.; Chang, P.; Fan, M.; Deng, J.; Xu, C. In situ growth of graphene catalyzed by a phase-change material at 400°C for wafer-scale optoelectronic device application. *Small* **2023**, *19* (14), No. 2206738.
(20) Wu, J.; Lu, Y.; Feng, S.; Wu, Z.; Lin, S.; Hao, Z.; Yao, T.; Li, X.; Zhu, H.; Lin, S. The interaction between quantum dots and graphene: the applications in graphene-based solar cells and photodetectors. *Adv. Funct. Mater.* **2018**, *28*, No. 1804712.
(21) Feng, S.; Dong, B.; Lu, Y.; Yin, L.; Wei, B.; Wang, J.; Lin, S. Graphene/p-AlGaN/p-GaN electron tunnelling light emitting diodes with high external quantum efficiency. *Nano Energy* **2019**, *60*, 836−840.
(22) Lung, Q.; Chu, R.; Kim, Y.; Laryn, T.; Madarang, M.; Kovalchuk, O.; Song, Y.; Lee, I.; Choi, C.; Choi, W.; Jung, D. Graphene/III−V Quantum Dot Mixed-Dimensional Heterostructure for Enhanced Radiative Recombinations via Hole Carrier Transfer. *Nano Lett.* **2023**, *23* (8), 3344−3351.
(23) Jang, L.; Jeon, D.; Kim, M.; Jeon, J.; Polyakov, A.; Ju, J.; Lee, S.; Baek, J.; Yang, J.; Lee, I. Investigation of Optical and Structural Stability of Localized Surface Plasmon Mediated Light-Emitting Diodes by Ag and Ag/SiO2 Nanoparticles. *Adv. Funct. Mater.* **2012**, *22*, 2728−2734.
(24) Kuo, Y.; Yang, C. Theoretical/Numerical Studies of the Nanoscale-Cavity Effects on Dipole Emission, Förster Resonance Energy Transfer, and Surface Plasmon Coupling. *Plasmonics* **2024**, *19*, 273−285.
(25) Lin, H.; Chen, Y.; Wu, J.; Wang, D.; Chen, C. Carrier transfer induced photoluminescence change in metal-semiconductor core-shell nanostructures. *Appl. Phys. Lett.*, **2006**, *88* (16), No. 161911.
(26) Sharma, S. N.; Pillai, Z. S.; Kamat, P. V. Photoinduced Charge Transfer between CdSe Quantum Dots and p-Phenylenediamine. *J. Phys. Chem. B* **2003**, *107* (37), 10088−10093.
(27) Wang, X.; Li, X. H.; Jiang, C.; Brown, C. T. A.; Ning, J. Q.; Zhang, K.; Yu, Q.; Ge, X. T.; Wang, Q. J.; Zhang, Z. Y. Photon-generated carrier transfer process from graphene to quantum dots: optical evidences and ultrafast photonics applications. *npj 2D Mater. Appl.* **2020**, *4*, 27.
(28) Huang, M.; Bakharev, P. V.; Wang, Z.-J.; Biswal, M.; Yang, Z.; Jin, S.; Wang, B.; Park, H. J.; Li, Y.; Qu, D.; Kwon, Y.; Chen, X.; Lee, S. H.; Willinger, M.-G.; Yoo, W. J.; Lee, Z.; Ruoff, R. S. Large-area single-crystal AB-bilayer and ABA-trilayer graphene grown on a Cu/Ni(111) foil. *Nat. Nanotechnol.* **2020**, *15*, 289−295.
(29) Gao, D.; Wang, L.; Su, X.; Pan, Y.; Li, S.; Han, X.; Wang, Y. Modulation of fluorescence radiation for ZnCdS/CdSe quantum dots by graphene at room temperature. *Appl. Surf. Sci.* **2020**, *526*, No. 146598.
(30) Ding, H.; Wei, J.-S.; Zhang, P.; Zhou, Z.-Y.; Gao, Q.-Y.; Xiong, H.-M. Solvent-Controlled Synthesis of Highly Luminescent Carbon Dots with a Wide Color Gamut and Narrowed Emission Peak Widths. *Small* **2018**, *14* (22), No. 1800612.
(31) Hola, K.; Sudolska, M.; Kalytchuk, S.; Nachtigallova, D.; Rogach, A. L.; Otyepka, M.; Zboril, R. Graphitic Nitrogen Triggers Red Fluorescence in Carbon Dots. *ACS Nano* **2017**, *11* (12), 12402−12410.




https://doi.org/10.1021/acsphotonics.5c01788
*ACS Photonics* 2025, 12, 6300−6307